


 Cite this: *RSC Adv.*, 2019, 9, 40681

# Antibacterial and thermomechanical properties of experimental dental resins containing quaternary ammonium monomers with two or four methacrylate groups

 Weiguo Wang,<sup>ID</sup> †<sup>a</sup> Sailing Zhu, †<sup>a</sup> Guoqing Zhang,<sup>a</sup> Fan Wu,<sup>a</sup> Jinghao Ban<sup>b</sup> and Limin Wang<sup>\*a</sup>

Resins with strong antibacterial and thermomechanical properties are critical for application in oral cavities. In this study, we first evaluated the antibacterial effect of an unfilled resin incorporating 1, 4, and 7 mass% of quaternary ammonium salt (QAS) monomers containing two methacrylate groups (MAE-DB) and four methacrylate groups (TMH-DB) against *Streptococcus mutans*, and tested the cytotoxicity and thermomechanical properties of the 4 mass% MAE-DB and TMH-DB modified resin materials. A neat resin without a QAS monomer served as the control. As the concentration of both QAS monomers increases, the formation of a *Streptococcus mutans* biofilm on the experimental material is increasingly inhibited. The results of colony forming unit counts and the metabolic activity showed that both the MAE-DB and TMH-DB modified resins have a strong bactericidal effect on the bacteria in a biofilm, but no bactericidal effect on the bacteria in a solution. The viability-staining and morphology results also demonstrate that the bacteria deform, lyse, shrink, and die on the surface of the two QAS-modified resins. Cytotoxicity results show that the addition of TMH-DB can reduce the cytotoxicity of the resin, while the addition of MAE-DB increases the cytotoxicity of the resin. DMA results show that a TMH-DB modified resin has a higher storage modulus than a MAE-DB modified resin owing to its better crosslink density. The two groups of experimental resins showed a similar glass transition temperature. These data indicate that the two QAS monomers can impart similar antibacterial properties upon contact with a dental resin, whereas TMH-DB can endow the resin with a higher crosslink density and storage modulus than MAE-DB because it has more polymerizable groups.

 Received 25th September 2019  
 Accepted 2nd December 2019

DOI: 10.1039/c9ra07788j

[rsc.li/rsc-advances](http://rsc.li/rsc-advances)

## 1. Introduction

Dental resin materials have become the main material for the filling treatment of caries owing to their superior esthetic results and simple handling properties. However, clinical investigations have shown less longevity for composite restorations compared with amalgam restorations.<sup>1</sup> Secondary caries are the main cause of the failure of dental resin restoration,<sup>2</sup> and occur significantly more frequently with the application of a dental resin than with an amalgam.<sup>3</sup> The retreatment of secondary caries costs the patient significant time and money, and may cause more serious consequences such as pulp and root tip infections. During the development of secondary caries, acidogenic and aciduric bacteria such as

*Streptococcus mutans* accumulate on the teeth and dental fillings, which can cause enamel and dentin demineralization through acid generation.<sup>4</sup> Following demineralization, degradation of the demineralized collagen matrix is induced by salivary proteases or endogenous peptidases, such as MMPs and cysteine cathepsins.<sup>5</sup> Therefore, secondary caries is a bacterial infectious disease, and endowing dental resin materials with antibacterial properties to reduce the bacterial adhesion to the resin materials is an important way to reduce such occurrence.

Previous methods for the antimicrobial modification of dental resins through a direct addition of soluble organic or inorganic antimicrobials have been gradually phased out owing to a susceptibility to the burst release effects of antimicrobials as well as their detrimental effects on the mechanical properties of the materials applied.<sup>6–10</sup> In recent years, some scholars have put forward strategies for using a polymerizable antibacterial agent to modify the antibacterial properties of dental resins.<sup>11–13</sup> A so-called polymerizable antibacterial agent is a type of material composed of an

<sup>a</sup>Department of Stomatology, No. 903 Hospital of PLA, Lingyin Road 14, Hangzhou, 310000, People's Republic of China. E-mail: wlm117@126.com; Fax: + 86 571 8734 0983; Tel: + 86 571 8734 0983

<sup>b</sup>School of Stomatology, Fourth Military Medical University, Xi'an, People's Republic of China

† These two authors contributed equally to this work as co-first authors.



antibacterial group and a polymerizable group. Owing not only to its stable antibacterial activity, but also its ability to generate a polymerization reaction, an antibacterial functional group can be firmly cross-linked and bound to the matrix material through a covalent bond, thus providing the matrix material with a stable antibacterial function independent of the release of the active ingredients.

At present, the vast majority of polymerizable antibacterial agents are based on quaternary ammonium salt (QAS) monomers containing methacrylate groups, in which methacrylate groups are used as polymerizable groups and quaternary ammonium groups are used as antibacterial groups. QAS monomer modified resins have been shown to have extremely strong antibacterial properties,<sup>9,14–16</sup> although their mechanical properties have decreased to varying degrees.<sup>17,18</sup> Monomethacrylate QAS monomers have been reported to incur a miscibility problem with commonly used dental monomers,<sup>19,20</sup> resulting in decreased mechanical properties of the resin. Although a dimethacrylate QAS monomer avoids the solubility problem, the mechanical properties of a dimethacrylate QAS monomer modified resin are still decreased owing to its low cross-linking degree with the resin matrix.<sup>21,22</sup> Both monomethacrylate QAS monomers and dimethacrylate QAS monomers are linear monomers, and their ability to cross-link to the resin matrix is limited. Jaymand *et al.* suggested that multi-functional and dendritic monomers can be used to improve the crosslinking degree and mechanical performance of the resin.<sup>23–25</sup> Compared to a linear monomer, monomers with multi-functional methacrylate groups provide an extremely high number of functional groups in a compact space with a high reactivity and can become a crosslinking center of the polymer.<sup>26</sup>

At present, few studies have been conducted on QAS monomers with multi-functional methacrylate groups, and there remains a lack of data regarding their comparison with linear QAS monomers. Therefore, in this study, we compared the effects of a new tetramethacrylate quaternary ammonium salt monomer (TMH-DB) and a dimethacrylate quaternary ammonium salt monomer (MAE-DB) with proven antibacterial properties for a resin modification, and analyzed their antibacterial and thermomechanical properties.

## 2. Experimental

### 2.1 Raw materials

The chemical structures of the different reactants are shown in Fig. 1. Bisphenol A glycerolate dimethacrylate (bis-GMA), tri(ethylene glycol) dimethacrylate (TEGDMA), camphorquinone (CQ), and ethyl 4-dimethylamino-benzoate (EDMAB) were purchased from Sigma-Aldrich (St. Louis, MO, USA). QAS antibacterial monomers (MAE-DB and TMH-DB), with the molecular formula shown in Fig. 1, were supplied by Xylmed Biomedical (Xi'an, China). All materials were used as received without further purification.

### 2.2 Experimental material preparation

The experimental resin comonomer was prepared at bis-GMA : TEGDMA weight ratios of 50 : 50. Next, 0.5% CQ and 1% EDMAB were added to the comonomer blends as the photo initiator and accelerator, respectively. All resin comonomer blends were homogenized and stored in the dark prior to use. Finally, TMH-DB and MAE-DB were added to the resin mixture. The groups and addition ratios are shown in Table 1. All resin mixture blends were also homogenized and stored in the dark prior to use.

### 2.3 Antibacterial activity test

**2.3.1 Preparation of polymerized resin specimens.** Experimental polymerized resin disks were fabricated using a cylindrical Teflon mold with an internal diameter of 10 mm and a height of 2 mm between two glass slides. The resin was polymerized for 60 s using a dental light source. The resin disks were then sterilized with ethylene oxide gas, followed by degassing for 48 h.

**2.3.2 Bacterial strain and culture conditions.** *Streptococcus mutans* (UA 159) was inoculated in a sterile brain heart infusion (BHI) broth (Difco, Becton-Dickinson and Co., Sparks, MD, USA) and cultured overnight at 37 °C in an anaerobic incubator. The resulting bacterial suspension was diluted to a concentration of  $1 \times 10^6$  colony forming units (CFUs) per mL for further use.

**2.3.3 Bacterial growth on material surfaces and in culture medium.** The sterile specimens were placed in the wells of a 24-

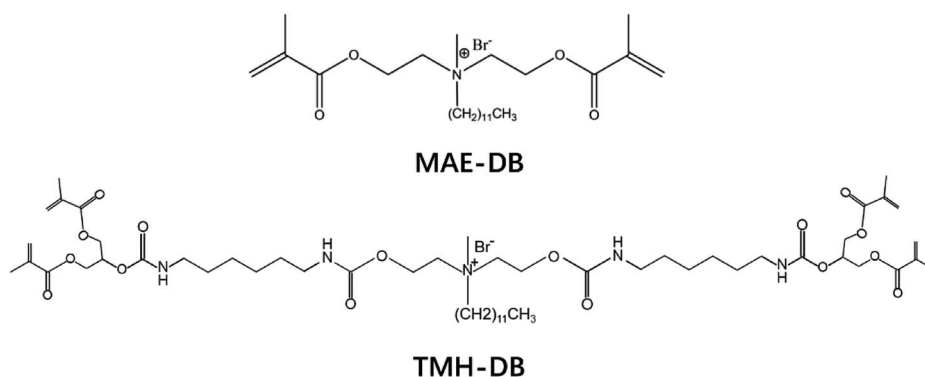


Fig. 1 Molecular formula of two quaternary ammonium salt monomers with different numbers of methacrylate groups.



Table 1 Compositions of the dental resin systems

Group	Resin	Composition of resin (wt%)		
		Neat resin mixture	TMH-DB	MAE-DB
NR	Neat resin	100	0	0
TB1	Resin with 1% TMH-DB	99	1	0
TB4	Resin with 4% TMH-DB	96	4	0
TB7	Resin with 7% TMH-DB	93	7	0
MB1	Resin with 1% MAE-DB	99	0	1
MB4	Resin with 4% MAE-DB	96	0	4
MB7	Resin with 7% MAE-DB	93	0	7

well plate with a 2 mL BHI broth. Then, 20 mL of a diluted *Streptococcus mutans* suspension was added to each well and incubated at 37 °C for 24 h under an anaerobic atmosphere to generate the biofilms. Specimens were taken out from the culture medium and washed twice with PBS and then transferred into a 15 mL sterile centrifuge tube with a 2 mL fresh BHI broth. Bacteria in the biofilm on the test piece surface were harvested through vortex mixing at a maximum speed for 2 min using a vortex mixer (Fisher Scientific, Pittsburgh, PA, USA). Once the specimens were removed from the wells, planktonic bacteria in the original medium samples were mixed thoroughly with repeated pipetting to achieve a homogeneous bacterial suspension.

The bacterial suspensions from both the biofilms on the disks and the planktonic bacteria in the medium were serially diluted, spread onto BHI agar plates, and incubated for 1 day at 5% CO<sub>2</sub> and 37 °C for a CFU analysis ( $n = 5$ ), following previously reported methods.<sup>27</sup>

**2.3.4 Bacterial metabolic activity on material surfaces and in a culture medium.** The bacterial suspensions obtained from biofilms and planktonic bacteria in the medium were prepared as described above. After a brief mixing using repeated pipetting, 200 µL of the bacterial suspensions were pipetted into a 96-well plate, and 20 µL of a cell counting kit-8 (CCK-8, APEX-BIO, USA) dye solution was then added to each well in turn and incubated anaerobically at 37 °C for 2 h. The absorbance of the solution in each well was then measured at 450 nm using a microplate reader (SpectraMax M5, Molecular Devices, USA).

**2.3.5 Scanning electron microscopy (SEM) of *Streptococcus mutans* on the tested material surfaces.** To each well of the 24-well plate, 2 mL of BHI broth and 20 µL of the diluted bacterial suspension were added and mixed thoroughly. Sterile disks were prepared for testing, placed in the wells, and anaerobically cultured at 37 °C for 24 h to form a biofilm. The disks coated with biofilms were then gently rinsed three times with sterile PBS to remove planktonic bacteria and the culture medium. In a new sterile 24-well plate, the specimens were soaked in 3% glutaraldehyde at 4 °C overnight, dehydrated in a graded series of ethanol solutions, and then dried in a critical-point drier. After a sputter coating of the samples with gold using an ion sputter (JFC-1100E, JEOL, Tokyo, Japan), all specimens were observed through a field emission SEM (FESEM; S-4800; Hitachi Ltd, Tokyo, Japan).

**2.3.6 Live/dead staining for visualization of *Streptococcus mutans* viability on material surfaces.** Specimens coated with a *Streptococcus mutans* biofilm were prepared as described above. The biofilm-coated disks were rinsed three times with sterile saline to remove any loose bacteria and then placed in a 24-well plate. Next, 1 mL of a Live/Dead Bac Light Bacterial Viability Kit L13152 (Molecular Probes, Invitrogen, Eugene, OR, USA) was added to each well to cover the sample, which was then incubated for 15 min at room temperature in the dark for fluorescent staining. Using this kit, live bacteria are stained using Syto 9, producing a green fluorescence, and bacteria with compromised membranes are stained by propidium iodide, producing a red fluorescence.<sup>27,28</sup> The stained samples were washed with sterile saline and observed using a laser confocal microscope under dual-channel scan mode. Excitation with a 488 nm laser showed a green fluorescence emission of the live bacteria, and excitation with a 543 nm laser showed a red fluorescence emission of bacteria with damaged membrane.

## 2.4 Cytotoxicity test

The material cytotoxicity was evaluated *via* an extraction method. Extracts were obtained from NR, TB4 and DB4 group incubated for 24 h at 37 °C in the Dulbecco's Modified Eagle's Medium (DMEM, GIBCO, BRL, Life Sciences, USA) containing 10% fetal calf serum (FCS). L929 mouse fibroblast cell was used to investigate cytotoxicity of the materials.

The real-time cell viability was assessed and monitored using a real-time cell analyzer (RTCA, xCELLigence system, ACEA Biosciences, Germany). The microbial suspension was added to each tube containing different resin extract. Cells exposed to DMEM containing 10% FCS without extract served as the control check (CK) group. RTCA was performed according to the supplier's instructions. The background impedance of the E-plate was determined by adding 50 µL culture medium or extract obtained during the previous step to each well and calculating automatically using the RTCA software, according to the following equation:  $C_1 = (Z_1 - Z_0)/15$ , where  $C_1$  is the cell index,  $Z_1$  is the impedance at any given time and  $Z_0$  is the background signal.<sup>29</sup> Subsequently, 150 µL cell suspension that contained 10<sup>4</sup> L929 mouse fibroblast cells was seeded in each well of the E-plate 96 and was allowed to settle at the bottom of the wells for 20 min before impedance measurements were performed at 15 min intervals.

## 2.5 Dynamic mechanical thermal analysis

Dynamic mechanical analysis (DMA) tests were conducted on a dynamic mechanical analyzer (DMA Q800, TA Instruments Co., USA) in three-point bending mode. Bar-shaped specimens (30 mm × 4 mm × 2 mm) were prepared in a Teflon mold and polymerized for 60 s using a dental light source. The specimens were stored in a 37 °C thermostatic container for 1 day and then used for DMA testing. The measurement was conducted within a temperature range of 0–250 °C at a frequency of 1 Hz (approximately the average chewing rate) with a heating rate of 5 °C min<sup>-1</sup>. The storage modulus and tan δ were plotted against the temperature over this period. The values of the storage



modulus at 37 °C ( $E'$ ) were recorded. The temperature at the maximum of the  $\tan \delta$  curve was taken as the glass transition temperature ( $T_g$ ). In addition, the crosslink density was calculated from the storage modulus in a rubbery plateau according to the rubber elasticity theory using the following equation:<sup>30,31</sup>

$$\nu = \frac{E''}{3\rho RT}$$

where  $\nu$  is the crosslink density (mol kg<sup>-1</sup>),  $E''$  is the storage modulus (MPa) at  $T_g + 30$  °C,  $\rho$  is the density (g mL<sup>-1</sup>),  $R$  is the gas constant (8.314472 J mol<sup>-1</sup> K<sup>-1</sup>), and  $T$  is the absolute temperature at  $T_g + 30$  °C.

## 2.6 Statistical analysis

One-way analyses of variance (ANOVAs) were conducted to detect the significant effects of the variables on the antibacterial and thermomechanical activities. Tukey's multiple comparison test was used to compare the differences between any two groups, with significance assumed at a  $p$ -value of 0.05.

## 3. Results

### 3.1 Antibacterial activity properties

**3.1.1 CFU counts of *Streptococcus mutans* on the surfaces of the tested materials and in the culture medium.** Table 2 shows the CFU counts of *Streptococcus mutans* on the surfaces of the tested materials. A statistical analysis shows that the concentration of a QAS monomer had a significant effect on the CFU count ( $p < 0.05$ ). As the proportion of MAE-DB and TMH-DB increased, the numbers of CFUs from the *Streptococcus mutans* biofilms on the resin presented an order of magnitude decrease. No significant difference was observed between the resins containing the same proportions of MAE-DB and TMH-DB ( $p > 0.05$ ). The CFU counts of planktonic *Streptococcus mutans* from the culture medium of the different tested materials are also listed in Table 2. MB7 had the lowest CFU count and was significantly different from the other groups ( $p < 0.05$ ). There were no significant differences in the CFU count of the remaining groups ( $p > 0.05$ ).

**3.1.2 Metabolic activity of *Streptococcus mutans* on the surfaces of the tested materials and in the culture medium.** The metabolic activity data for *Streptococcus mutans* biofilms on the material surfaces are plotted in Fig. 2. The results show that the

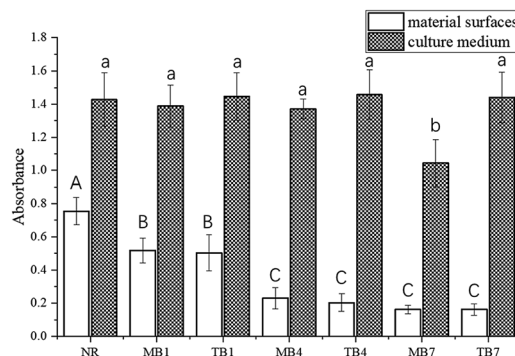


Fig. 2 Metabolic activity of *Streptococcus mutans* on material surfaces and in culture medium. Higher absorbance values represent more metabolically viable bacteria. Values with dissimilar letters are significantly different from each other ( $p < 0.05$ ). Values with the same letter are not significantly different ( $p > 0.05$ ).

NR group had the highest metabolic activity of bacteria in the biofilm, which was significantly higher than all QAS modified resin groups ( $p < 0.05$ ). No significant differences were observed between the resins containing the same proportions of MAE-DB and TMH-DB ( $p > 0.05$ ). The metabolic activity of bacteria within the biofilms of MB1 and TB1 was significantly less than that of the other QAS modified resin groups ( $p < 0.05$ ). No significant difference in metabolic activity was observed among the MB4, MB7, TB4, and TB7 groups ( $p > 0.05$ ). The metabolic activity data for planktonic *Streptococcus mutans* in the culture medium of all experimental groups except for the MB7 group also showed no statistical difference ( $p > 0.05$ ). The activity of the MB7 group was significantly lower than that of the other groups, however ( $p < 0.05$ ).

**3.1.3 SEM imaging of *Streptococcus mutans* on the tested material surfaces.** Representative SEM images of the adherence of *Streptococcus mutans* biofilms on the polymerized resin disks after 24 h of anaerobic culturing are collectively shown in Fig. 3. Thick biofilms with a multi-layered three-dimensional structure appear on the NR surface. The biofilm thickness and bacteria area of the experimental resins decreased with increases in the MAE-DB and TMH-DB concentration. Lysed or shrunken bacteria cells can be observed in the higher magnitude images of the

Table 2 CFU counts from *Streptococcus mutans* on material surfaces and in culture medium<sup>a</sup>

Group	CFU (per disk) on material surfaces	CFU (per mL) in culture medium
NR	$7.09(0.52) \times 10^7$ A	$7.6(0.59) \times 10^8$ A
MB1	$6.15(0.71) \times 10^6$ B	$7.4(0.82) \times 10^8$ A
TB1	$5.19(0.68) \times 10^6$ B	$7.1(0.44) \times 10^8$ A
MB4	$6.86(0.42) \times 10^4$ C	$6.9(0.53) \times 10^8$ A
TB4	$6.44(0.67) \times 10^4$ C	$7(0.58) \times 10^8$ A
MB7	$4.12(0.65) \times 10^3$ D	$5.6(0.67) \times 10^8$ B
TB7	$3.71(0.92) \times 10^3$ D	$6.9(0.63) \times 10^8$ A

<sup>a</sup> CFU values represent the mean (SD) of five replicates. Values with the same superscript letter are not significantly different ( $p > 0.05$ ).



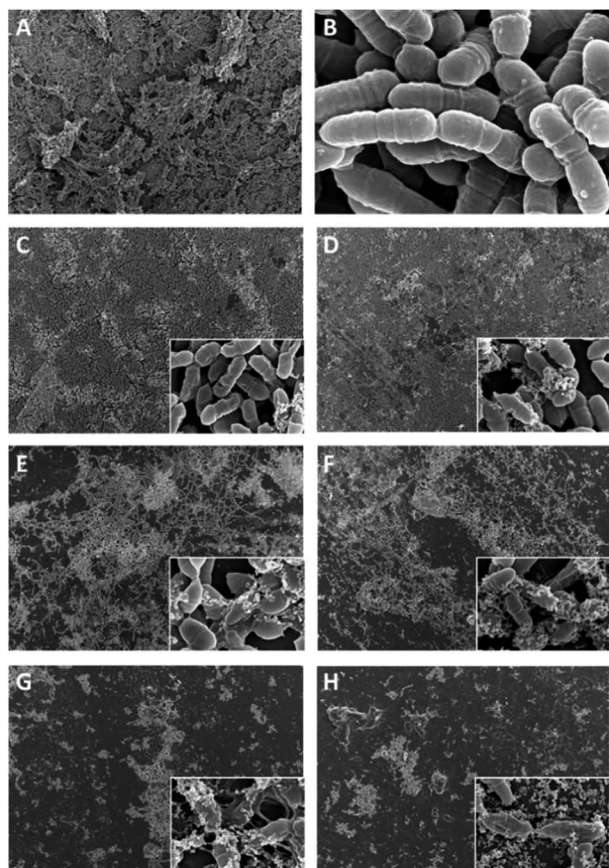


Fig. 3 Representative SEM images of *Streptococcus mutans* biofilms on experimental resin surfaces after 24 h of aerobic growth in BHI medium: (A) lower magnification micrographs (1000 $\times$ ) of NR, (B) higher magnification micrographs (50 000 $\times$ ) of NR, (C) MB1, (D) TB1, (E) MB4, (F) TB4, (G) MB7, and (H) TB7.

experimental resins, and increased with increasing concentrations of the MAE-DB and TMH-DB. Experimental resins with different concentrations of MAE-DB and TMH-DB were able to disturb the integrity of the bacteria and cause a lysis of the bacterial cells, showing similarly strong antibacterial properties.

**3.1.4 Viability of *Streptococcus mutans* on the tested material surfaces.** Representative CLSM images of biofilms with a live/dead stain are shown in Fig. 4. The two QAS monomer modified resins demonstrated similar antibacterial properties. As the QAS concentration increased, the number of viable bacteria decreased, whereas the number of dead bacteria increased, and almost no viable bacteria were present on the surfaces of the TB7 and MB7 groups.

### 3.2 Cytotoxicity properties

Fig. 5 illustrates that as the culture time increased, the number of cells increased slowly owing to cell proliferation. During the first five days of culture, the cell indices of the NR, TB4, and MB4 groups were smaller than that of CK group, and the cell index of the TB4 group was higher than that of the NR and MB4 groups.

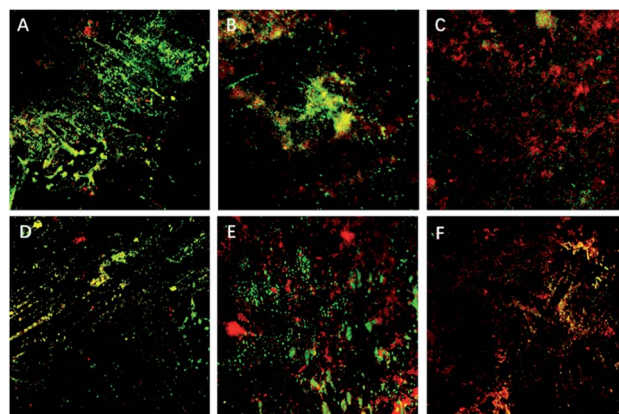


Fig. 4 Representative CLSM images of live/dead-stained biofilms on material surfaces. Representative CLSM images of live/dead-stained biofilms after 24 h of anaerobic growth on the tested material surfaces: (A) MB1, (B) MB4, (C) MB7, (D) TB1, (E) TB4, and (F) TB7. Live bacteria exhibited green fluorescence, and bacteria with compromised membranes exhibited red fluorescence.

### 3.3 Dynamic mechanical thermal properties

The curves of the storage modulus *versus* temperature and  $\tan \delta$  *versus* temperature are shown in Fig. 6, and Table 3 lists the values of the storage modulus at 37  $^{\circ}\text{C}$  ( $E$ ), glass transition temperature ( $T_g$ ), and crosslink density ( $\nu$ ). With an increase in temperature,  $E$  decreased continuously and reached a plateau at approximately 190  $^{\circ}\text{C}$ . The curves of  $\tan \delta$  *versus* temperature present a unimodal structure.

The MB4 group had similar  $E$  and  $\nu$  values as the NR group, and no differences in the statistical comparison could be seen. The TB4 group had the highest  $E$ , which was significantly higher than that of the NR4 and MB4 groups. The TB4 group had the largest  $\nu$ , which was significantly higher than that of the MB4 group, whereas it was not statistically different from the NR group. The three groups of experimental resins showed a similar  $T_g$  with no statistical difference.

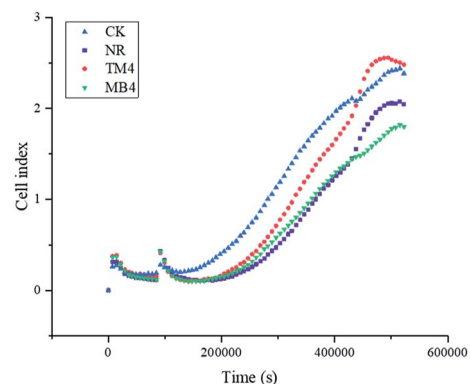


Fig. 5 Real-time monitoring of L929 cells exposed to different resin extracts using a real-time cell analyzer.



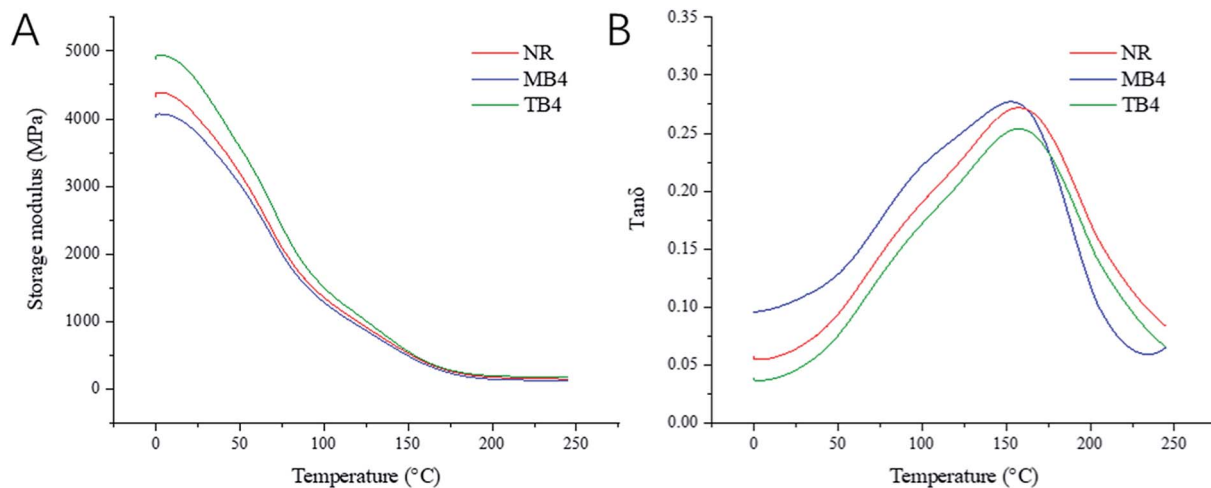


Fig. 6 Representative curves of (A) storage modulus versus temperature and (B)  $\tan \delta$  versus temperature of dental resins.

Table 3 Storage modulus at 37 °C ( $E$ ), glass transition temperature ( $T_g$ ), and crosslink density ( $\nu$ ) of experimental dental resins<sup>a</sup>

Resins	$E$ (MPa)	$T_g$ (°C)	$\nu$ (mol kg <sup>-1</sup> )
NR	3570.3 ± 141.9 <sup>A</sup>	158.9 ± 3.6 <sup>A</sup>	33.82 ± 2.55 <sup>AB</sup>
MB4	3593.3 ± 124.6 <sup>A</sup>	158.5 ± 1.9 <sup>A</sup>	31.97 ± 0.9 <sup>A</sup>
TB4	4051.3 ± 56.4 <sup>B</sup>	156.6 ± 5.2 <sup>A</sup>	36.77 ± 1.03 <sup>B</sup>

<sup>a</sup> Different uppercase letters represent statistically significant differences in same column ( $P < 0.05$ ).

## 4. Discussion

Dental caries is an infectious disease that depends on the presence of bacterial biofilms, which are a specialized bacterial community formed by bacteria and their extracellular macromolecules. Such films have a special spatial structure and can produce a strong barrier to resist the bactericidal effect of antibiotics.<sup>32</sup> Bacteria in biofilms are about 500-times more tolerant to antimicrobial components compared to planktonic bacteria,<sup>33</sup> which is mainly because the antimicrobial component binds to the exopolysaccharide in the biofilm matrix, making it difficult to penetrate inside the mature biofilm.<sup>34</sup> In addition, the bacteria in the biofilm can communicate and transmit resistance genes.<sup>35</sup>

Therefore, the tolerance of the microorganisms in biofilms to antimicrobials has been an important issue. Bacteria adhesion is an essential step in the formation of biofilms on biomaterial surfaces, and involves an initial instantaneous physicochemical phase, followed by a time-dependent molecular and cellular phase.<sup>35</sup> Thus, limiting the bacterial adhesion is an effective way to prevent bacterial biofilm maturation.

*Streptococcus mutans* is a major pathogen causing human dental caries,<sup>36</sup> and was therefore chosen for an evaluation of the antibacterial effects of the materials prepared in this study. It plays an important role in the initial adhesion, and produces glucosyltransferase and subsequently synthesizes glucan *in situ*

to provide binding sites for cariogenic microorganisms and promote the maturation of biofilms.<sup>37</sup> The present study investigated the antibacterial activity of experimental resins containing MAE-DB and TMH-DB monomers on *Streptococcus mutans*, both on the surface and in a solution around the surface. The results show that all experimental groups except MB7 inhibited the *Streptococcus mutans* biofilm growth and metabolic activity on the surface but had no effect on the bacteria in the solution, which is a very good characteristic for dental resin materials. The experimental resins have strong bactericidal and bacteriostatic effects upon contact with *Streptococcus mutans* in biofilms, which can inhibit the initial adhesion of bacteria on the resin surface and prevent the formation of mature biofilms. By contrast, the experimental resins showed no bactericidal effect on the planktonic *Streptococcus mutans* in the culture medium, indicating that the quaternary ammonium salt monomer did not penetrate into the culture medium, and that the antibacterial effect of the experimental resins does not depend on the release of antibacterial molecules. Therefore, the physical and chemical properties and biosafety of the resin matrix will not be reduced owing to the monomer release. The MB7 group inhibited *Streptococcus mutans* biofilm growth and metabolic activity while also inhibiting planktonic *Streptococcus mutans* growth and metabolic activity, which indicates that MAE-DB infiltrated into the medium. This may be due to MAE-DB being a linear monomer and the fact that it cannot be completely covalently bound to the resin matrix when the amount of MAE-DB added to the resin exceeds a certain limit, resulting in the residual monomer in the resin matrix.

SEM results showed that both QAS-modified resins had significant and similar antibacterial properties, and that the antibacterial effect increased with the increase in the QAS monomer concentration. When the concentration of both types of QAS was 1%, the structure of the bacterial biofilm became thin and the morphology of the bacteria changed. However, when the concentration of both types of QAS was more than 4%, the bacteria could not form complete biofilms on the resin



surface, and numerous lysed or shrunken bacteria and bacterial debris appeared. CLSM also showed similar results, and with an increase in the QAS concentration, the antimicrobial properties of the modified resin continuously increased, the number of viable bacteria decreased, and the number of dead bacteria increased. The antibacterial properties of QAS monomers are based on the cationic immobilization mechanism.<sup>38</sup> They mainly rely on positively charged quaternary ammonium groups to attract negatively charged bacteria. After contact with bacteria, long-chain alkyl groups in quaternary ammonium salt monomers can penetrate the cell wall and react with the phospholipid bilayer in the cell membrane, destroying the cell membrane structure, leading to cytoplasmic exposure and causing bacterial death.<sup>17</sup> Thus, QAS monomers are dependent on kill-on-contact microbiocidal activities that can limit the biofilm maturation by reducing the bacterial adhesion and killing adventitious bacteria.

The membrane components of eukaryotic cells are similar to bacteria, and they are mainly composed of phospholipid bilayers. In theory, quaternary ammonium salts also cause damage to eukaryotic cells, including human cells. In addition, the polymerizable methacrylate groups in the quaternary ammonium salt monomers may also be another source of its cytotoxicity. Polymerizable methacrylate groups are characteristic groups of dental monomers, and studies have shown that conventional dental methacrylate monomers also have a certain degree of cytotoxicity.<sup>39</sup> The results of real-time cell analysis showed that DB4 group had the lowest cell index; while the cell index of TB4 group were still smaller than CK group, but better than NR group. So, it can be concluded from this study that the addition of TMH-DB can reduce the cytotoxicity of the resin, while the addition of MAE-DB increases the cytotoxicity of the resin.

The mechanical properties of dental composite resin materials have traditionally been measured using a static method. However, a dental composite resin shows a viscoelastic behavior owing to the presence of a resin matrix (polymer), which is more suitable for a dynamic mechanical analysis. A dynamic thermomechanical analysis (DMA) is used to measure the mechanical properties of viscoelastic materials as a function of time, temperature, or frequency when subjected to cyclic (sinusoidal) mechanical stresses. DMA can better simulate the cyclic masticatory loading under a large temperature difference to which dental resins are clinically subjected.<sup>40</sup> This can be extremely valuable for predicting the clinical performance of dental resin materials in human physiological motion.<sup>31</sup> The two groups of 4% QAS-modified resins showed significant antibacterial properties, and thus in this study, TM4 and MB4 were used in a DMA to test their thermomechanical properties.

Dental resins are used as rigid materials in an oral cavity. It is therefore desirable for dental resins to have a sufficient elastic modulus to maintain their shape stability. Strictly speaking, although an elastic modulus is not the same as a storage modulus, both have similar values during glassy and rubber states for crosslinked networks with a high crosslink density. The storage modulus mainly depends on the flexibility of molecular segments and the temperature conditions. The size

of a resin network depends on the number of chemical bonds that are crosslinked between the polymer branches. After a crosslinking of the polymer, the rotation and movement of the molecule are greatly restricted, and the rigidity and mechanical properties of the resins are associated with the crosslink density of the network.<sup>41</sup> This study showed that the TB4 group had the highest  $E$ , which was mainly due to its highest crosslink density. A high crosslink density leads to a decrease of the free volume in the resin matrix and the strengthening of the rigidity of the molecular segments, which has a stronger impeding effect on the movement of the molecular segments of the resin. The crosslink density of the MB4 group was not significantly different from that of the NR group, resulting in  $E$  also not being significantly different from that of the NR group. The higher crosslink density of TMH-DB than MAE-DB is due TMH-DB having a higher number of functional end groups. In dental resins, the higher crosslink density of a multifunctional monomer provides a sufficient number of bridges between linear macromolecules, resulting in certain benefits, such as a three-dimensional network, thereby improving the mechanical properties and melting temperature of the resin.<sup>25</sup>

$\tan \delta$  indicates the damping and is a measure of how well a material disperses energy in its mass. A high  $\tan \delta$  indicates a high molecular mobility of the material, whereas a low  $\tan \delta$  indicates a low mobility. It is known that the storage of composites at 37 °C will induce some post curing, and that the  $\tan \delta$  curve also changes from bimodal to unimodal.<sup>42</sup> The temperature corresponding to the maximum value of the  $\tan \delta$  curve is  $T_g$ , and all three groups of experimental resins have only one  $T_g$ , which is the critical transition temperature of the polymer material from a glassy to a rubbery state, during which the mechanical properties such as the strength and modulus of the polymer material will significantly change. The crosslinking, densification, and decrease in the flexibility of a molecular chain lead to a movement of  $T_g$  toward a high temperature, whereas the breakage and increase in flexibility of a molecular chain lead to the movement of  $T_g$  toward a low temperature. For methacrylate resin, which belongs to amorphous polymer materials,  $T_g$  is the upper limit temperature for its use, and is a key technical parameter for characterizing the heat resistance of a dental resin. The results show that there was no significant difference in  $T_g$  among the three groups, and  $T_g$  was significantly higher than the temperature that can be endured in the mouth, indicating that the addition of TMH-DB and MAE-DB does not adversely affect the thermodynamic properties of the resin.

## 5. Conclusions

In summary, this study indicated that the incorporation of TMH-DB and MAE-DB endow dental resins with similar strong antibacterial effects against *Streptococcus mutans* and can therefore play an important role in preventing the occurrence of secondary caries. The multifunctional QAS monomer TMH-DB has more polymerizable groups than the bifunctional QAS monomer MAE-DB, which can form a denser cross-linked network with a resin matrix and thus has a higher cross-



linking density and less cytotoxicity. Thus, we suggest that TMH-DB is a more promising candidate for incorporation in a dental resin.

## Conflicts of interest

The authors state no conflict of interest.

## Acknowledgements

This work was supported financially by the National Natural Science Foundation of China (81600916, 81701030).

## References

- 1 M. Alhareky and M. Tavares, *J. Evid. Based Dent. Pract.*, 2016, **16**, 107–109.
- 2 Á. Ástvaldsdóttir, J. Dagerhamn, J. W. V. van Dijken, A. Naimi-Akbar, G. Sandborgh-Englund, S. Tranæus and M. Nilsson, *J. Dent.*, 2015, **43**, 934–954.
- 3 I. Nedeljkovic, W. Teughels, J. De Munck, B. Van Meerbeek and K. L. Van Landuyt, *Dent. Mater.*, 2015, **31**, e247–e277.
- 4 P. Totiam, C. González-Cabezas, M. R. Fontana and D. T. Zero, *Caries Res.*, 2007, **41**, 467–473.
- 5 L. Tjäderhane, M. A. R. Buzalaf, M. Carrilho and C. Chaussain, *Caries Res.*, 2015, **49**, 193–208.
- 6 G. do Amaral, T. Negrini, M. Maltz and R. Arthur, *Aust. Dent. J.*, 2016, **61**, 6–15.
- 7 A. M. Young, in *Drug-Device Combination Products*, Elsevier, 2010, pp. 246–279.
- 8 R. S. Tobias, *Int. Endod. J.*, 2007, **21**, 155–160.
- 9 L. Chen, H. Shen and B. I. Suh, *Am. J. Dent.*, 2012, **25**, 337–346.
- 10 N. Beyth, S. Farah, A. J. Domb and E. I. Weiss, *React. Funct. Polym.*, 2014, **75**, 81–88.
- 11 N. Zhang, K. Zhang, X. Xie, Z. Dai, Z. Zhao, S. Imazato, Y. A. Al-Dulaijan, F. D. Al-Qarni, M. D. Weir, M. A. Reynolds, Y. Bai, L. Wang and H. H. K. Xu, *Nanomaterials*, 2018, **8**, 393.
- 12 S. Imazato and J. F. McCabe, *J. Dent. Res.*, 1994, **73**, 1641–1645.
- 13 Y. Ge, S. Wang, X. Zhou, H. Wang, H. H. K. Xu and L. Cheng, *Materials*, 2015, **8**, 3532–3549.
- 14 S. Imazato, R. R. B. Russell and J. F. McCabe, *J. Dent.*, 1995, **23**, 177–181.
- 15 L. Huang, F. Yu, X. Sun, Y. Dong, P. Lin, H. Yu, Y. Xiao, Z. Chai, X. Xing and J. Chen, *Sci. Rep.*, 2016, **6**, 33858.
- 16 L. Cheng, M. D. Weir, K. Zhang, S. M. Xu, Q. Chen, X. Zhou and H. H. K. Xu, *J. Dent. Res.*, 2012, **91**, 460–466.
- 17 Y. Jiao, L. Niu, S. Ma, J. Li, F. R. Tay and J. Chen, *Prog. Polym. Sci.*, 2017, **71**, 53–90.
- 18 W. Zhu, C. Lao, S. Luo, F. Liu, Q. Huang, J. He and Z. Lin, *J. Biomater. Sci. Polym. Ed.*, 2018, **29**, 635–645.
- 19 N. Ebi, S. Imazato, Y. Noiri and S. Ebisu, *Dent. Mater.*, 2001, **17**, 485–491.
- 20 J. He, E. Söderling, L. V. J. Lassila and P. K. Vallittu, *Dent. Mater.*, 2012, **28**, e110–e117.
- 21 X. Liang, E. Söderling, F. Liu, J. He, L. V. J. Lassila and P. K. Vallittu, *J. Mater. Sci. Mater. Med.*, 2014, **25**, 1387–1393.
- 22 J. He, E. Söderling, L. V. J. Lassila and P. K. Vallittu, *Dent. Mater.*, 2014, **30**, 968–976.
- 23 M. Jaymand, M. Lotfi, J. Barar and S. Kimyai, *Res. Chem. Intermed.*, 2017, **43**, 5707–5722.
- 24 M. Jaymand, M. Lotfi and M. Abbasian, *Mater. Res. Express*, 2018, **5**, 035406.
- 25 M. Jaymand, M. Lotfi and R. Lotfi, *RSC Adv.*, 2016, **6**, 43127–43146.
- 26 L. G. Schultz, Y. Zhao and S. C. Zimmerman, *Angew Chem. Int. Ed. Engl.*, 2001, **40**, 1962–1966.
- 27 Y. Yang, L. Huang, Y. Dong, H. Zhang, W. Zhou, J. Ban, J. Wei, Y. Liu, J. Gao and J. Chen, *PLoS One*, 2014, **9**, e112549.
- 28 L. Huang, F. Yu, X. Sun, Y. Dong, P. Lin, H. Yu, Y. Xiao, Z. Chai, X. Xing and J. Chen, *Sci. Rep.*, 2016, **6**, 33858.
- 29 H. Benachour, T. Bastogne, M. Toussaint, Y. Chemli, A. Sève, C. Frochot, F. Lux, O. Tillement, R. Vanderesse and M. Barberi-Heyob, *PLoS One*, 2012, **7**, e48617.
- 30 L. C. Yamasaki, A. G. De Vito Moraes, M. Barros, S. Lewis, C. Francci, J. W. Stansbury and C. S. Pfeifer, *Dent. Mater.*, 2013, **29**, e169–e179.
- 31 S. Luo, F. Liu and J. He, *J. Mech. Behav. Biomed. Mater.*, 2019, **94**, 222–228.
- 32 T.-F. Mah, *Future Microbiol.*, 2012, **7**, 1061–1072.
- 33 T.-F. C. Mah and G. A. O'Toole, *Trends Microbiol.*, 2001, **9**, 34–39.
- 34 H. Ishida, Y. Ishida, Y. Kurosaka, T. Otani, K. Sato and H. Kobayashi, *Antimicrob. Agents Chemother.*, 1998, **42**, 1641–1645.
- 35 U. Obst, T. Schwartz and H. Volkmann, *Int. J. Artif. Organs*, 2006, **29**, 387–394.
- 36 L. Liu, T. Hao, Z. Xie, G. P. Horsman and Y. Chen, *Sci. Rep.*, 2016, **6**, 37479.
- 37 W. H. Bowen and H. Koo, *Caries Res.*, 2011, **45**, 69–86.
- 38 S. Liu, L. Tonggu, L. Niu, S. Gong, B. Fan, L. Wang, J. Zhao, C. Huang, D. H. Pashley and F. R. Tay, *Sci. Rep.*, 2016, **6**, 21882.
- 39 Y. Pei, H. Liu, Y. Yang, Y. Yang, Y. Jiao, F. R. Tay and J. Chen, *Oxid. Med. Cell. Longevity*, 2018, **2018**, 1–14.
- 40 E. C. Vouvoudi and I. D. Sideridou, *J. Mech. Behav. Biomed. Mater.*, 2012, **10**, 87–96.
- 41 L. C. Yamasaki, A. G. De Vito Moraes, M. Barros, S. Lewis, C. Francci, J. W. Stansbury and C. S. Pfeifer, *Dent. Mater.*, 2013, **29**, e169–e179.
- 42 I. D. Sideridou and M. M. Karabela, *J. Appl. Polym. Sci.*, 2008, **110**, 507–516.

